Subsurface Sensing Technologies and Applications, Vol. 6, No. 1, January 2005 (© 2005)
DOI: 10.1007/s11220-005-4228-x

Frequency Dependence of the Soil Electromagnetic Properties Derived from Ground-Penetrating Radar Signal Inversion

Sébastien Lambot[1,2,*], Idesbald van den Bosch[3], Benoit Stockbroeckx[4], Pascal Druyts[5], Marnik Vanclooster[2], and Evert Slob[1]

[1]Department of Geotechnology, Delft University of Technology, Mijnbouwstraat 120, 2628 RX Delft, The Netherlands
[2]Department of Environmental Sciences and Land Use Planning, Catholic University of Louvain, Louvain-la-Neuve, Belgium
[3]Microwave Laboratory, Catholic University of Louvain, Louvain-la-Neuve, Belgium
[4]Mic6 Company, Louvain-la-Neuve, Belgium
[5] Signal and Image Center, Royal Military Academy, Brussels, Belgium

Received October 22, 2004; revised February 1, 2005

The accuracy at which the subsurface electromagnetic properties can be identified from full wave inversion of ground penetrating radar (GPR) signals relies on the appropriateness of the model describing their frequency dependence. In this paper, we focus on the characterization of the frequency dependence of the dielectric permittivity and electric conductivity of a sandy soil subject to different water contents from inversion of GPR measurements. Based on previous studies of Lambot *et al.* the methodology relies on an ultrawide band (UWB) stepped-frequency continuous-wave (SFCW) radar combined with an off-ground monostatic transverse electromagnetic (TEM) horn antenna. Forward modeling of the radar signal is based on linear system transfer functions for describing the antenna, and on the exact solution of Maxwell's equations for wave propagation in a horizontally multilayered medium representing the subsurface. Model inversion, formulated by the classical least-squares problem, is carried out iteratively using advanced global optimization techniques. The frequency dependence of the electromagnetic properties of the sandy soil is characterized by performing inversions of the radar signal in different and subsequent limited frequency bands, in which the electromagnetic parameters are assumed to be constant. We observed that over the entire frequency band considered in this study (1–3 GHz), the dielectric permittivity of the

*To whom all correspondence should be addressed. Phone: 31-15-278 6028; fax: 31-15-2781189; e-mail: s.lambot@citg.tudelft.nl

sand remains constant with frequency, whatever the water content is. In contrast, the electric conductivity increases significantly from 1GHz to 3 GHz, and this effect increases with water content. The frequency dependence of the electric conductivity may be adequately described using a simple linear relationship. This approach is advantageous since it limits the number of parameters to be optimized in the inverse modeling procedure.

Key Words. Ground penetrating radar, soil electromagnetic properties, inverse modeling, frequency dependence.

1. Introduction

The soil electromagnetic properties are essential variables in agricultural and environmental engineering because they permit to identify using non-destructive measurement methods the soil water and chemical contents that control plant growth, hydrological processes, and the contamination of surface and subsurface water. The knowledge of the soil electromagnetic properties is also important in diverse civil and military engineering applications, and in particular in humanitarian demining for which they can be determinant regarding the performances of landmine sensors. It has become evident that modeling detailed spatial distributions and dynamics of the soil properties in the inherently heterogeneous subsurface requires extensive site characterization [1]. Characterizing this variability with conventional methods is invasive and thus, time-consuming, costly, and subject to a large degree of uncertainty due to the lack of densely sampled *in situ* measurements.

Ground penetrating radar (GPR) can be used for non-destructive characterization of the hydrogeophysical properties of the subsurface. However, notwithstanding the considerable research that has been devoted to GPR, its use for assessing quantitatively the subsurface properties is still constrained by the lack of appropriate GPR techniques. The GPR has been used to identify soil stratigraphy [2], to locate the water table [3], to monitor wetting front movement [4], to measure soil water content through dielectric permittivity [5–8], to assist in subsurface hydraulic parameter identification [9], to assess soil electric conductivity and salinity [10], and also to support the monitoring of contaminants [11]. An excellent review on GPR methods for measuring soil dielectric permittivity and water content is given by Huisman *et al.* [12].

The main limitations of the existing GPR characterization methods arise from the commonly used strongly simplifying assumptions with respect to the antenna radiation properties and electromagnetic wave propagation phenomena. As a result, only a part of the information contained in the GPR signal is utilized, usually the propagation time. Additionally, commercially available GPR systems have generally a bandwidth less than

1 GHz. A larger bandwidth is needed for a better spatial resolution and to acquire more information from the ground [13].

To circumvent the limitations of the existing methods, Lambot *et al.* [14,15] recently proposed a new promising integrated approach relying on full wave inverse modeling. It is based on an ultrawide band (UWB) stepped-frequency continuous-wave (SFCW) radar combined with an off-ground monostatic antenna. This radar configuration enables high mobility, to acquire more information from the ground due to the large bandwidth, and allows further for a realistic, accurate, and efficient forward and inverse modeling of the radar signal. The radar-antenna-subsurface system is modeled using linear system transfer functions and the exact solution of the three-dimensional (3-D) Maxwell's equations for wave propagation in a horizontally multilayered medium. The inversion to identify the subsurface properties, namely, the dielectric permittivity and electric conductivity, is formulated by the classical least-squares problem and is carried out iteratively using the global multilevel coordinate search optimization algorithm combined sequentially with the local Nelder–Mead simplex algorithm [16,17].

An important issue in the inverse modeling procedure is the assumption of an appropriate model for describing the frequency dependence of the soil electromagnetic properties. Only a few studies investigate frequency dispersion in the GPR frequency band [18]. In this study, we extend the work reported by Lambot *et al.* [15] by characterizing experimentally in controlled laboratory conditions the frequency dependence of the electromagnetic properties of a sandy soil using GPR, across the frequency range 1–3 GHz. This provides valuable insights regarding the parameterization of the inverse modeling procedure, in which the number of parameters to be optimized should be limited given the strong non-linearity of the inverse electromagnetic problem. The electromagnetic parameter extraction method used in this study has been validated in Lambot *et al.* [15].

2. Ground Penetrating Radar System

In this paper we used an UWB SFCW radar that is emulated using a vector network analyzer (VNA) (ZVRE, Rohde & Schwarz). The antenna consists of a linear polarized double-ridged broadband transverse electromagnetic (TEM) horn antenna (BBHA 9120 D, Schwarzbeck Mess-Elektronik) that is used off-ground in monostatic mode, i.e., the same antenna serves as emitter and receiver. This radar configuration possesses several advantages over commonly used time domain technologies and bi-static antenna systems [13]. The main advantages are: (1) the potential for controlling an UWB signal, which is necessary for a high depth resolution

and to obtain a maximum of information from the subsurface; (2) the higher signal-to-noise ratio of SFCW radars, due to the higher mean radiated power; (3) the wider dynamic range; (4) and the focused beaming of the TEM horn yielding high horizontal resolution and high soil response when operating with the ground situated in the far-field of the antenna, which results in important forward modeling simplifications.

3. Forward Modeling

3.1. Antenna Equation in the Frequency Domain

Assuming that the soil surface is in the Fraunhofer region (far-field) of the antenna, the antenna can be modeled accurately as a point source and receiver [19]. Moreover, given a monostatic configuration, antenna modeling does not require knowledge of the source radiation pattern, since the measured signal has only propagated along the antenna's axial direction, when the subsurface is assumed to be locally a horizontally multilayered medium. Consequently, the antenna being a causal time-invariant linear system, it can be modeled as a simple linear system composed of elementary model components in series and parallel, each characterized by its own frequency response function accounting for a specific electromagnetic phenomenon. The antenna is modeled using the block diagram represented in Figure 1 [15]. The resulting transfer function, expressed in the frequency domain, is given by

$$S_{11}(\omega) = \frac{b(\omega)}{a(\omega)} = H_{\mathrm{i}}(\omega) + \frac{H_{\mathrm{t}}(\omega) G_{\mathrm{xx}}^{\uparrow}(\omega) H_{r}(\omega)}{1 - H_{\mathrm{f}}(\omega) G_{\mathrm{xx}}^{\uparrow}(\omega)}, \tag{1}$$

where $S_{11}(\omega)$ is the quantity measured by the VNA; $b(\omega)$ and $a(\omega)$ are, respectively, the received and emitted waves at the VNA reference calibration plane; $H_{\mathrm{i}}(\omega)$, $H_{\mathrm{t}}(\omega)$, $H_{\mathrm{r}}(\omega)$, and $H_{\mathrm{f}}(\omega)$ are, respectively, the complex return loss, transmitting, receiving, and feedback loss transfer functions of the antenna; $G_{\mathrm{xx}}^{\uparrow}(\omega)$ is the transfer function of the air-subsurface system modeled as a horizontally multilayered medium; and ω is the angular frequency.

Defining $H(\omega) = H_{\mathrm{t}}(\omega) H_{\mathrm{r}}(\omega)$, the antenna is characterized by three transfer functions. These can be determined accurately over the entire frequency range by solving a system of equations as (1), pertaining to different model configurations. The simplest way is to consider measurements with the antenna located at different heights above a metal sheet, for which the model configurations are well known, and therefore, for which the Green's functions can readily be computed.

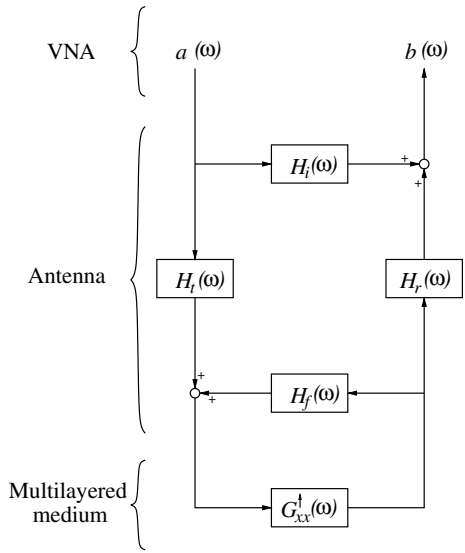

Figure 1. Block diagram representing the VNA-antenna-multilayered medium system modeled as linear systems in series and parallel.

3.2. Subsurface Model

Given the monostatic configuration and the focused beaming of the antenna, the measured radar signal has mainly propagated in the vertical antenna axial direction. As a result, the horizontal variability of the electromagnetic properties inherently encountered in environmental systems is expected to play a negligible role, and the ground can be modeled realistically and efficiently using a horizontally multilayered configuration, as depicted in Figure 2. The model is 3-D and consists of N horizontal layers separated by $N-1$ interfaces. The medium of the Nth layer is homogeneous and characterized by the dielectric permittivity ε_n, electric conductivity σ_n, and thickness h_n. The magnetic permeability is assumed to be equal to the permeability of free space. The source and receiver point is located in the upper half-space, representing the air layer. The emitting part of the TEM horn is approximated by an infinitesimal horizontal x-directed electric dipole, whereas the receiving part of the antenna is emulated by recording the horizontal x-directed component of the backscattered (upward) electric field.

For this configuration, closed form analytical expressions can be derived for the exact solution of the system of Maxwell's equations. Following the approach of Slob and Fokkema [20], we compute the

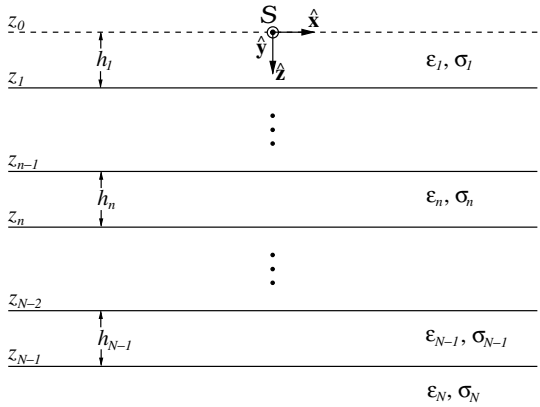

Figure 2. Model configuration: 3-D N-layered medium with a point source S.

air-subsurface transfer Green function, $G^{\uparrow}_{xx}(\omega)$, i.e., the solution of Maxwell's equations, by computing recursively the transverse electric and magnetic global reflection coefficients of the multilayered system in the 2-D spatial Fourier domain. It is worth noting that the 3-D model is essential to account for spherical divergence in electromagnetic wave propagation.

3.3. Frequency Dependence of the Soil Electromagnetic Properties

It is well known that in the operating frequency range of GPR, soil materials can exhibit significant dispersive properties, i.e., the electromagnetic properties of the soil are function of frequency e.g., [18]. At these frequencies, dispersion arises mainly from relaxation mechanisms due to the presence of water, water bound to mineral surfaces (bound water and double layer polarization effects), and interactions between ions and soil particles (Maxwell–Wagner effect).

To have a realistic model of propagation of electromagnetic waves in the lossy subsurface, it is therefore necessary to account for these effects. The frequency dependence is usually described with the empirical extended Debye relaxation equation [21], which involves a single relaxation phenomenon. Yet, in reality, the electromagnetic properties of most subsurface materials contains more than one relaxation mechanism due to the presence of water, granular mixtures, etc. In this case, a volumetric mixing model that sums two or more dielectric spectra with different Debye parameters may describe dielectric dispersion of soils more realistically than Debye equation [22].

However, over the limited frequency range of GPR, it is unrealistic to identify all these multiple parameters simply from inversion of the radar signal. The inverse problem would be ill-posed due to non-linearity, poor sensitivities, and parameter correlations. For this reason, in the study of Lambot *et al.* [15] dealing with a sandy soil, the frequency dependence of the dielectric permittivity was assumed to be negligible, and the frequency dependence of the electric permittivity was assumed to be described by the linear equation

$$\sigma(f) = \sigma_{1\,\mathrm{GHz}} + a\left(f - 10^9\right), \tag{2}$$

where $\sigma_{1\,\mathrm{GHz}}$ is the reference apparent electric conductivity at 1 GHz, and a is the linear variation rate of $\sigma(f)$. This relation was assumed to be a reasonable local approximation of the frequency dependence over the frequency range 1–2 GHz, and is validated in this study for the sandy soil in the range 1–3 GHz.

4. Model Inversion

In the particular case where no prior information on the parameters is taken into account and assuming observation errors to be an independent zero mean stationary Gaussian process, the maximum likelihood theory reduces to the weighted least-squares problem. The objective function to be minimized is accordingly defined as follows

$$\Phi(\mathbf{b}) = \left|G_{\mathrm{xx}}^{\uparrow *}(\omega) - G_{xx}^{\uparrow}(\omega, \mathbf{b})\right|^T \frac{1}{\sigma^2} \left|G_{\mathrm{xx}}^{\uparrow *}(\omega) - G_{xx}^{\uparrow}(\omega, \mathbf{b})\right|, \tag{3}$$

where $G_{\mathrm{xx}}^{\uparrow *}(\omega)$ and $G_{\mathrm{xx}}^{\uparrow}(\omega, \mathbf{b})$ are the vectors containing, respectively, the observed and simulated response functions of the multilayered medium, and σ^2 is the error variance. Since these response functions are complex functions, the difference between observed and modeled data is expressed by the amplitude of the errors in the complex plane. As in most electromagnetic inverse problems, this error function is highly non-linear and is characterized by an oscillatory behavior and a multitude of local minima. This complex topography necessitates the use of a robust global optimization algorithm. We use the global multilevel coordinate search algorithm [16] combined sequentially with the classical Nelder–Mead simplex algorithm [17].

In this paper, the frequency dependence of the soil electromagnetic properties is investigated in two ways. First, as in Lambot *et al.* [15], inversions are performed in the entire frequency band (i.e., 1–3 GHz) by considering the dielectric permittivity to be constant with frequency,

and the electric conductivity to follow relation (2). Second, inversions are performed in different and subsequent limited frequency ranges, in which both the dielectric permittivity and electric conductivity are assumed to be constant. The entire frequency range has been divided in five subbands of 400 MHz as follows: 1.0–1.4, 1.4–1.8, 1.8–2.2, 2.2–2.6, and 2.6–3.0 GHz. Dividing the whole frequency range in smaller bands leads to unrealistic values for the inversely estimated parameters, since the limited information is then not sufficient to ensure stability of the inverse solution in relation to measurement and modeling errors. This is illustrated below by the response surface analysis.

5. Laboratory Experiments

5.1. Experimental Setup

Radar measurements were carried out in controlled laboratory conditions on a tank filled with a single sand layer (see Fig. 3) subject to different water contents, denoted $W1 = 0.031$, $W2 = 0.083$, $W3 = 0.123$, $W4 = 0.144$, $W5 = 0.152$, $W6 = 0.181$, and $W7 = 0.194\,\mathrm{m^3\,m^{-3}}$. Water content values at the GPR measurement scale were inferred from the dielectric permittivites obtained from signal inversions in the whole frequency range using the soil specific relationship derived in Lambot *et al.* [15] for the same material. The thickness of the sand layer was

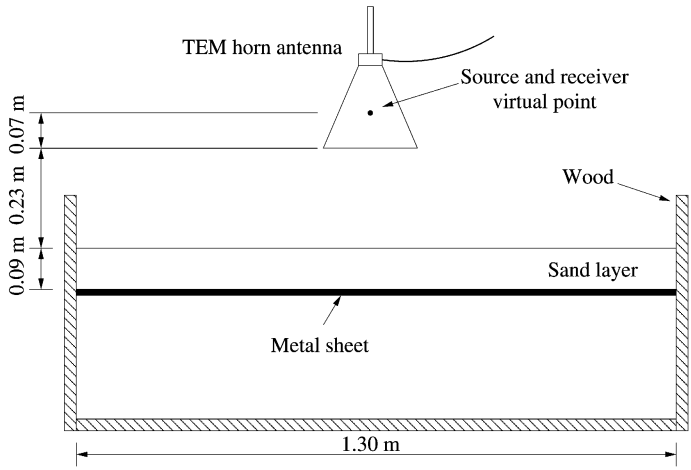

Figure 3. Laboratory experimental setup including the sand box made of wood, the off-ground TEM horn antenna, the sand layer, and the metal sheet to control the bottom boundary condition in the electromagnetic model.

equal to about 9 cm. A horizontal metal sheet was installed to control the bottom boundary conditions in the electromagnetic model. Indeed, laboratory materials underneath this metal sheet have no influence on the measured backscattered signal. The antenna was located at about 23 cm above the sand surface, which is far below the far-field limit (estimated at 0.51 m at 3 GHz and assuming the largest dimension of the antenna at its virtual source point). However, experiments demonstrated that the far-field assumption is not a critical hypothesis in the electromagnetic model. The advantage of being closer to the sand surface in the laboratory is that the assumption of an infinite horizontally multilayered medium for the sand box is less violated due to the smaller antenna foot print, and it also improves the signal-to-noise ratio, since less energy is lost through spherical divergence. Parameter $S_{11}(\omega)$ was measured sequentially over the range 1–3 GHz with a frequency step of 8 MHz.

5.2. Frequency Dependence of the Dielectric Permittivity

Figure 4 represents the measured and modeled Green's function for the $W4$ water content level. Results are comparable for other water contents. Data are presented in both the frequency and time domains. Compared to the study of Lambot *et al.* [15], the measured Green's function is very well reproduced by the electromagnetic model, because now we use an over-determined system of equations given in (1) to obtain the system transfer functions much more accurately than in the previous study. A second reason is that now the antenna is located closer to the sand surface, which is possible without deteriorating the model results. In the time domain, we recognize the reflection on the sand surface, around 2 ns, and the reflection on the metal sheet, around 3.5 ns.

Inversion results for the dielectric permittivity are presented in Figure 5. We can observe from inversions performed in the sub-frequency bands that in the frequency range 1–3 GHz, the dielectric permittivity of the sand does not show significant frequency dispersion, whatever the water content is. Moreover, results are in close agreement with inversions performed in the entire frequency range. Differences arise from the larger effect of the measurement and modeling errors on the value of the inversely estimated parameters when only a limited frequency range is considered. It is worth noting that for some scenarios, inversions performed in the sub-frequency bands led to unrealistic values, which are not shown on Figure 5. We verified that the optimization algorithm did not converge to a local solution, but that the global minimum was at an unrealistic position due to instability (see response surface analysis).

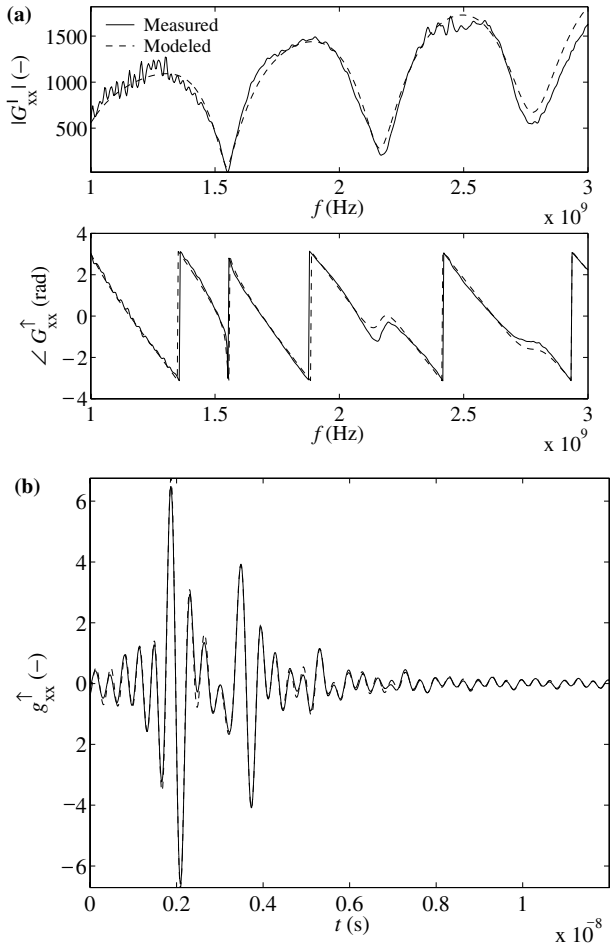

Figure 4. Measured and modeled Green's function for the $W4$ water content level. Data are presented in both the frequency (a) and time domains (b).

5.3. Frequency Dependence of the Electric Conductivity

Similarly, inversion results for the electric conductivity of the sand are presented in Figure 6. First, in accordance with Eq. (2), inversions performed in the entire frequency range show a significant frequency dependence of the electric conductivity between 1 GHz and 3 GHz (parameter a in (2) is not negligible). The value of the estimated electric conductivity at 3 GHz is generally more than twice the value at 1 GHz. It is also worth noting that the frequency dependence increases with water content, which

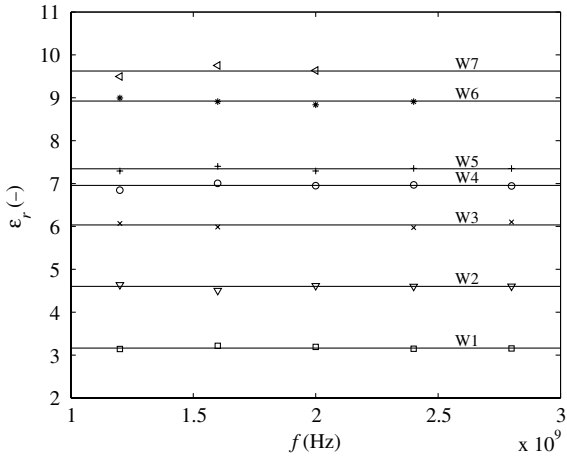

Figure 5. Frequency dependence of the relative dielectric permittivity for the different water contents. Solid lines represent the constant model for inversion in the entire frequency band (1–3 GHz), and markers represent the constant model for inversions in different subsequent frequency bands (1.0–1.4, 1.4–1.8, 1.8–2.2, 2.2–2.6, and 2.6–3.0 GHz).

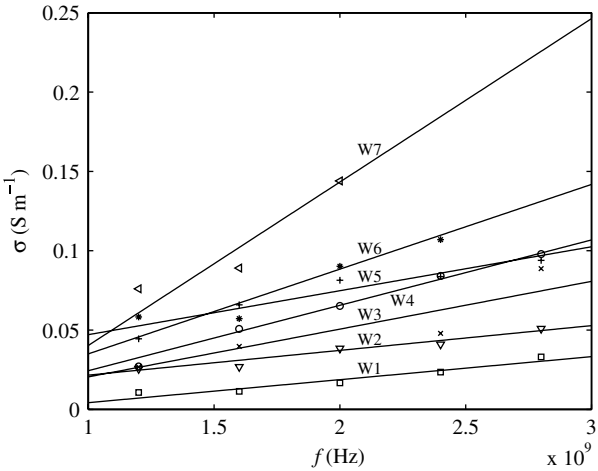

Figure 6. Frequency dependence of the electric conductivity for the different water contents. Solid lines represent the linear model for inversion in the entire frequency band (1–3 GHz), and markers represent the constant model for inversions in different subsequent frequency bands (1.0–1.4, 1.4–1.8, 1.8–2.2, 2.2–2.6, and 2.6–3.0 GHz).

emphasizes the important role of water in frequency dispersion and relaxation phenomena.

Markers represent independent inversion results when considering the five subsequent frequency bands. We can observe that the results correspond remarkably well with the linear model presented in Eq. (2). However, discrepancies between the two approaches are more important than for the dielectric permittivity. This is to be attributed to the limited sensitivity of the Green's function to the electric conductivity as compared to the dielectric permittivity in the considered parameter space (see [14]). This results in a higher instability of the inverse estimation in relation to measurement and modeling errors.

Finally, note that the results obtained for the water content level $W5$ are not consistent with other water contents, although the two optimization approaches are consistent. The origin of this difference has not been elucidated but may be attributed to various factors such a casual temperature variation effect, heterogeneity of the sand properties, a different geometric arrangement of the sand grains, or a particular distribution of water in the pore space at this water content.

5.4. Response Surface Analysis

Uniqueness and stability of the inverse solution can be investigated using response surfaces of the objective function which partially reveal the presence of a well-defined solution, occurrence of local minima and also qualitatively parameter sensitivities and correlations. Response surfaces are 2-D contour plots representing the objective function as a function of two parameters, while all other parameters are kept constant at their true value.

Figure 7 represents response surfaces pertaining to the $W4$ case, considering three different frequency bands of decreasing bandwidth, namely, 1.0–3.0, 1.8–2.2, and 1.8–2.0 GHz. For the larger bandwidth (2 GHz, Fig. 7(a)), we observe the presence of a well-defined global minimum. The Green's function is less sensitive to the electric conductivity than to the dielectric permittivity in the considered parameter space. The two parameters are not significantly correlated. When bandwidth is reduced to 400 MHz (Fig. 7(b)), the global minimum is slightly different, and two local minima appear. Uniqueness and stability requirements are however still satisfied. Then, if bandwidth is limited to 200 MHz (Fig. 7(c)), we can observe that the two previously observed local minima become deeper, and one replaces the global minimum which is no more at a correct position. This results in unrealistic values for the optimized parameters, and indicates that if bandwidth is to small compared to measurement and modeling errors, the inverse solution is not stable any more.

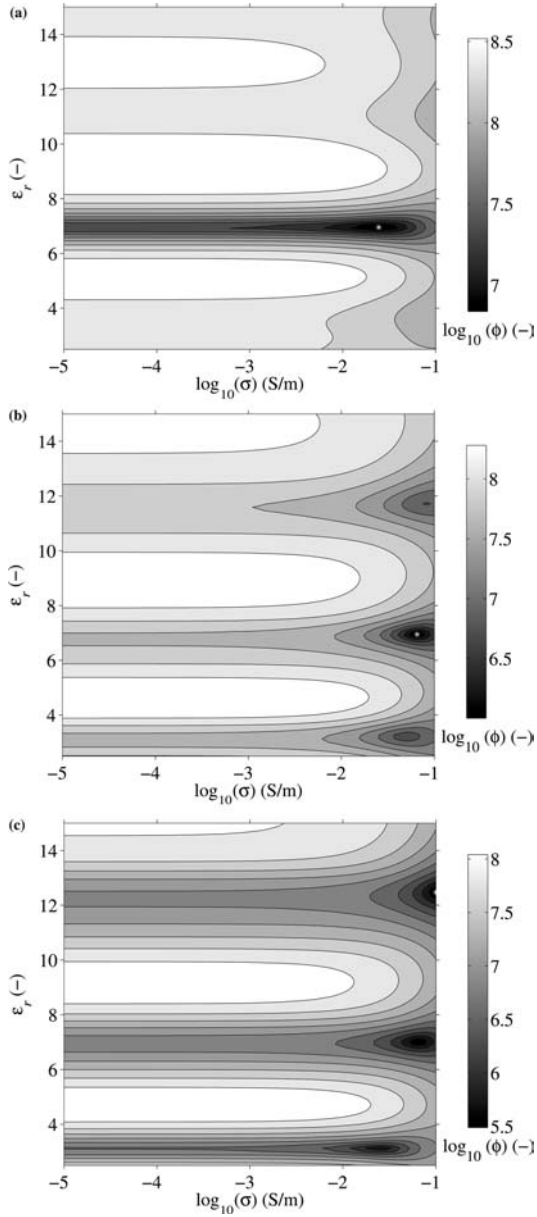

Figure 7. Objective function response surfaces pertaining to the *W*4 case, considering three different frequency bands of decreasing bandwidth, namely, 1.0–3.0 GHz (a), 1.8–2.2 GHz (b), and 1.8–2.0 GHz (c). The star represents the global minimum of the objective function.

6. Conclusions

In this paper, we used the approach of Lambot *et al.* [15] to investigate using GPR signal full wave inverse modeling the frequency dependence of the electromagnetic properties of a sandy soil subject to a range of different water contents. The soil dielectric properties are therefore characterized in an effective way at the macroscopic GPR characterization scale. We observed that over the entire frequency band considered in this study (1 GHz to 3 GHz), the dielectric permittivity of the sand remains independent of frequency, whatever the water content is. In contrast, the electric conductivity increases significantly from 1–3 GHz, and this effect increases with water content. The frequency dependence of the electric conductivity may be adequately described using a simple linear relationship. A linear model is advantageous since it limits the number of parameters to be optimized in the inverse modeling procedure. Finally, it is worth noting that we observed that the far-field condition in the electromagnetic model is not critical, and very good results can be obtained with the antenna relatively close to the ground (23 cm in this study).

Further studies will focus on the dielectric characterization of other soil types (loamy and clayey soils), and on a better understanding of the fundamental mechanisms governing frequency dispersion in the GPR frequency range.

Acknowledgments

This research was supported by a Marie-Curie Intra-European Fellowships within the 6th European Community Framework Programme, the FNRS (Belgium), the Catholic University of Louvain (Belgium), the Royal Military Academy (Belgium), and Delft University of Technology (The Netherlands).

References

1. Yeh, T.-C.J., Gelhar, L.W., and Gutjahr, A.L., 1985, Stochastic analysis of unsaturated flow in hetergogeneous soils, 1, Statistically isotropic media, Water Resour. Res., v. 21, p. 447–456.
2. Davis, J.L. and Annan, A.P., 1989, Ground penetrating radar for high resolution mapping of soil and rock stratigraphy. Geophys. Prospecting, v. 37, p. 531–551.
3. Nakashima Y., Zhou H., and Sato M., 2001, Estimation of groundwater level by GPR in an area with multiple ambiguous reflections. J. Appl. Geophys., v. 47, p. 241–249.
4. Vellidis, G., Smith, M.C., Thomas, D.L., and Asmussen, L.E., 1990, Detecting wetting front movement in a sandy soil with ground penetrating radar, Trans. ASAE, v. 33, p. 1867–1874.

5. Chanzy, A., Tarussov, A., Judge, A., and Bonn, F., 1996, Soil water content determination using digital ground penetrating radar. Soil Sci. Soci. Ame. J., v. 60, p. 1318–1326.
6. Weiler, K.W., Steenhuis, T.S., Boll, J., and Kung, K.-J.S., 1998, Comparison of ground penetrating radar and time domain reflectometry as soil water sensors. Soil Sci. Soc. Am. J., v. 62, p. 1237–1239.
7. Huisman, J.A., Sperl, C., Bouten, W., and Verstraten, J.M., 2001, Soil water content measurements at different scales: Accuracy of time domain reflectometry and ground penetrating radar. J. Hydrol., v. 245, p. 48–58.
8. Serbin, G. and Or, D., 2003, Near-surface water content measurements using horn antenna radar: methodology and overview. Vadose Zone, 2, p. 500–510.
9. Hubbard, S.S., Rubin, Y., and Majer, E., 1997, Ground-penetrating-radar-assisted saturation and permeability estimation in bimodal systems. Water Resour. Res., v. 33, p. 971–990.
10. al Hagrey, S.A. and Müller, C., 2000, GPR study of pore water content and salinity in sand. Geophysical Prospecting, v. 48, p. 63–85.
11. Yoder, R.E., Freeland, R.S., Ammons, J.T., and Leonard, L.L., 2001, Mapping agricultural fields with GPR and EMI to identify offsite movement of agrochemicals. J. Appl. Geophy, v. 47, p. 251–259.
12. Huisman, J.A., Hubbard, S.S., Redman, J.D., and Annan, A.P., 2003, Measuring soil water content with ground penetrating radar: A review. Vadose Zone J., v. 2, p. 476–491.
13. Daniels, D.J., 1995 Surface Penetrating Radar, The Inst. Electrical Eng, London.
14. Lambot, S., Slob, E.C., van den Bosch, I., Stockbroeckx, B., Scheers, B., and Vanclooster, M., 2004a, Estimating soil electric properties from monostatic ground-penetrating radar signal inversion in the frequency domain. Water Resou. Res., 40, W04205, 14 doi:10.1029/2003WR002095.
15. Lambot, S., Slob E.C., van den Bosch, I., Stockbroeckx, B., and Vanclooster, M., 2004b., Modeling of ground penetrating radar for accurate characterization of subsurface dielectric properties. IEEE Transactions on Geoscience and Remote Sensing, v. 42, p. 2555–2568, 2004.
16. Huyer, W. and Neumaier, A., 1999, Global optimization by multilevel coordinate search. J. of Global Optimiz., v. 14, p. 331–355.
17. Lambot, S., Javaux, M., Hupet, F., and Vanclooster, M., 2002, A global multilevel coordinate search procedure for estimating the unsaturated soil hydraulic properties. Water Resour Res., 38, 1224, doi:10.1029/2001WR001224.
18. West, L.J., Handley, K., Huang, Y., and Pokar, M., 2003, Radar frequency dielectric dispersion in sandstone: Implications for determination of moisture and clay content. Water resour. Res., 39, 1026, doi:10.1029/2001WR000923.
19. Balanis, C.A., 1997., Antenna Theory: Analysis and Design., J. Wiley, New York.
20. Slob, E.C. and Fokkema, J., 2002, Coupling effects of two electric dipoles on an interface. Radio Sci 37, 1073, doi:10.1029/2001RS2529.
21. Debye, P., 1929, Polar Molecules: Reinhold, New York.
22. Heimovaara, T., Bouten, W., and Verstraten, J., 1994 Frequency domain analysis of time domain reflectometry waveforms, 2, A four-component complex dielectric mixing model for soils. Water Resour. Res., v. 30, p. 201–209.